Asociación Argentina
de Mecánica Computacional

Mecánica Computacional Vol XXVI, pp.1788-1799
Sergio A. Elaskar, Elvio A. Pilotta, Germán A. Torres (Eds.)
Córdoba, Argentina, Octubre 2007

NONLINEAR PDE SYSTEM AS MODEL OF AVASCULAR TUMOR GROWTH

D. Fernández Slezak[a], A. Soba[a], C. Suárez[a], M. Risk[a] and G. Marshall[a]

[a]*Laboratorio de Sistemas Complejos, Departamento de computación, Facultad de Ciencias Exactas y Naturales, Universidad de Buenos Aires, Ciudad Universitaria, Pabellón I, (C1428EGA) Buenos Aires, Argentina.*

Abstract.

In this paper we present the solution of a partial differential equation system to model avascular tumors growth. A detailed finite-difference numeric algorithm for solving the whole system is presented. The system, that includes moving boundary condition and a two-point boundary equation, is solved using a predictor-corrector scheme. The model is sensitive to the used numerical method, so a second-order accurate algorithm is necessary rather than a standard first-order accuracy one. A contracting mesh is also used in order to obtain the solution, as rate of change gets significantly high near tumor bound. Parameters are swiped to cover a wide range of feasible physiological values. Previous published works have taken into account the use of a single set of parameter values; therefore a single curve was calculated. In contrast, we present a range of feasible solutions for tumor growth, covering a more realistic scenario. A dynamical analysis and local behavior of the system is done. Chaotic situations arise for particular set of parameter values, showing interesting fixed points where biological experiments may be triggered.

1 INTRODUCTION

The mathematics dedicated to the resolution of oncologic problems, called "oncologic mathematics", is considered a new specialty in the interdisciplines Preziosi (2003); Byrne et al. (2006) and it is based in the utilization of mathematical methods and models for the description and prediction of morphologic and physiologic aspects of the tumor development. Ward & King's models Ward and King (1997, 1999, 2003) describe the growth or regression of an avascular microtumor versus the nutrient and/or drug concentration present in the medium. These models can be experimentally applied to and validated by the biological model of multicellular spheroids.

The model described in this paper is based on a system of nonlinear partial differential equations which assumes the existence of a continuum of cells in two possible states: alive or dead. According to the concentration of a generic nutrient, the living cell may reproduce or die. Besides, the external drug application can be modeled as a presence of a material able to diffuse to the spheroid interior and to kill cells with linear or Michaelis-Menten kinetics. The division or death of cells implies the expansion or contraction of the tumor volume, respectively, with the consequent generation of an associated velocity field.

2 MODEL EQUATIONS

The model equations were first presented in Ward and King (1997) and have basically three unknowns:

- living cells (n);
- local velocity of tumor cells (v);
- nutrient concentration (c).

These three unknowns depend on time and space with the following equations:

$$\frac{\partial n}{\partial t} + \nabla \cdot (vn) = [k_m(c) - k_d(c)]n \tag{1}$$

$$\nabla \cdot v = k_m(c) n V_L - k_d(c) n (V_L - V_D) \tag{2}$$

$$\frac{\partial c}{\partial t} + \nabla \cdot (vc) = \nabla \cdot (D \nabla c) - [\beta k_m(c) + \gamma(c)]n \tag{3}$$

where k_m y k_d are the mitosis and cellular death ratios respectively; V_L and V_D the living and dead cell volume; γ the nutrient consumption rate of a cell in interphase; and β the nutrient consumption rate of a cell in mitosis.

$$k_m(c) = \frac{A c^{m_1}}{c_c^{m_1} + c^{m_1}}$$
$$k_d(c) = B \left(1 - \frac{\sigma c^{m_2}}{c_d^{m_2} + c^{m_2}} \right)$$

where c_c is the critical concentration for cell proliferation, c_d the critical concentration for cell survival and σ the basal rate of cell death without nutrient limitations. In figure 1 we show k_m and k_d for different values of m_1 and m_2.

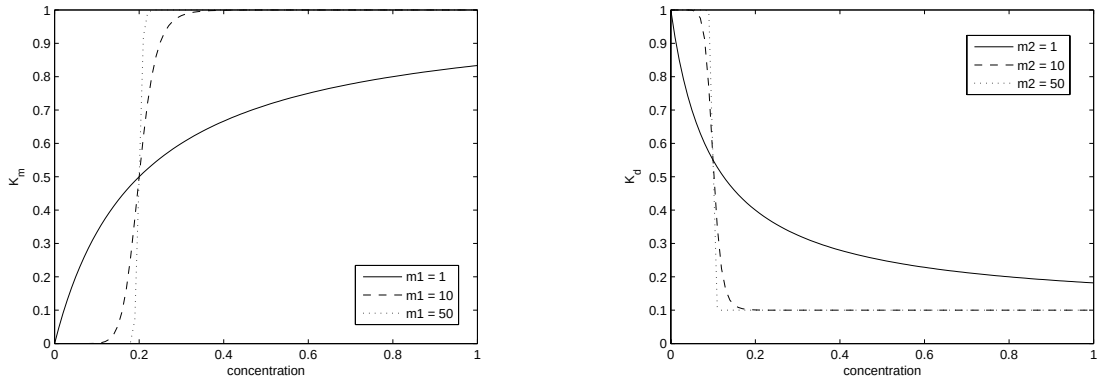

Figure 1: k_m and k_d functions, with $A = B = 1$, $\sigma = 0.9$, $c_c = 0.2$ Casciari et al. (1992); Hlatky et al. (1988) and $c_d = 0.1$. The figure shows that k_m and k_d tend to a Heaviside function when $m_1 \to \infty$.

2.1 Initial and boundary conditions

Boundary conditions considered are the tumour radius $S(t)$, the outer nutrient concentration, the velocity at the center of the tumor and a smoothness condition:

$$\frac{\partial S}{\partial t} = v(t, S(t)), \qquad c(t, S(t)) = c_0 \tag{4}$$

$$\frac{\partial c(t,0)}{\partial r} = 0, \qquad v(t,0) = 0 \tag{5}$$

Initial conditions are represented by a unique cell submerged in a given nutrient concentration:

$$S(0) = \sqrt[3]{\frac{3}{4\pi} V_L}, \qquad n(0,r) = \frac{1}{V_L}, \qquad c(0,r) = c_0 \tag{6}$$

3 NUMERICAL SOLUTION

For solving the model presented in section 2, we first exploit the spherical symmetry of the problem and then apply the non-dimensionalization.

3.1 Spherical Symmetry and Non-dimensionalization

We will denote a dimensionless variable with a hat (for example, $\hat{n}$). The dimensionless variables are:

$$n = \hat{n}/V_L \qquad c = c_0\hat{c} \qquad t = \hat{t}/A \qquad r = r_0\hat{r} \qquad v = Ar_0\hat{v} \qquad S = r_0\hat{S} \qquad \text{with } r_0 = S(0)$$

The non-dimensionalization and the spherical symmetry leads to the following equations system:

$$\frac{\partial \hat{n}}{\partial \hat{t}} + \hat{v}\frac{\partial \hat{n}}{\partial \hat{r}} = [a(\hat{c}) - b(\hat{c})\hat{n}]\hat{n} \tag{7}$$

$$\frac{1}{\hat{r}^2}\frac{\partial(\hat{r}^2\hat{v})}{\partial \hat{r}} = b(\hat{c})\hat{n} \tag{8}$$

$$\nu\left(\frac{\partial\hat{c}}{\partial\hat{t}}+\hat{v}\frac{\partial\hat{c}}{\partial\hat{r}}+b(\hat{c})\hat{c}\hat{n}\right)=\frac{1}{\hat{r}^2}\frac{\partial}{\partial\hat{r}}\left(\hat{r}^2\frac{\partial\hat{c}}{\partial\hat{r}}\right)-k(\hat{c})\hat{n} \tag{9}$$

where

$$\hat{k}_m(\hat{c})=\frac{\hat{c}^{m_1}}{\hat{c}^{m_1}+\hat{c}_c^{m_1}},\qquad \hat{k}_d(\hat{c})=\frac{B}{A}\left(1-\sigma\frac{\hat{c}^{m_2}}{\hat{c}^{m_2}+\hat{c}_d^{m_2}}\right) \tag{10}$$

$$a(\hat{c})=\hat{k}_m(\hat{c})-\hat{k}_d(\hat{c}) \tag{11}$$

$$b(\hat{c})=\hat{k}_m(\hat{c})-(1-\delta)\hat{k}_d(\hat{c})=a(\hat{c})+\delta\hat{k}_d(\hat{c}) \tag{12}$$

$$k(\hat{c})=\hat{\beta}\hat{k}_m(\hat{c})+\hat{\gamma}(\hat{c}) \tag{13}$$

where $\delta = V_D/V_L \in [0,1]$, $\hat{\beta} = r_0^2\beta A/DV_Lc_0$, $\hat{\gamma}(\hat{c}) = r_0^2\gamma(c)/DV_Lc_0$, $\hat{c}_c = c_c/c_0$, $\hat{c}_d = c_d/c_0$ and $\nu = Ar_0^2/D$. $a(\hat{c})$ represents the rate of cell population growth, $b(\hat{c})$ the rate of volume growth and $k(\hat{c})$ is proportional to the nutrient consumption of the system.

Taking into account that $\nu \approx 10^{-5}$ and $time\_unit \approx 14$ hours, we can rewrite equation 9 assuming the quasi-steady approximation as:

$$\frac{1}{\hat{r}^2}\frac{\partial}{\partial\hat{r}}\left(\hat{r}^2\frac{\partial\hat{c}}{\partial\hat{r}}\right)=k(\hat{c})\hat{n} \tag{14}$$

For the symmetric dimensionless system, the boundary conditions are:

$$\frac{\partial\hat{S}}{\partial\hat{t}}=\hat{v}(\hat{t},\hat{S}(\hat{t})),\qquad \hat{c}(\hat{t},\hat{S}(\hat{t}))=1 \tag{15}$$

$$\frac{\partial\hat{c}(\hat{t},0)}{\partial\hat{r}}=0,\qquad \hat{v}(\hat{t},0)=0 \tag{16}$$

$$\hat{n}(\hat{t},\hat{S}(\hat{t}))=\frac{a(1)e^{a(1)\hat{t}}}{a(1)-b(1)(1-e^{a(1)\hat{t}})} \tag{17}$$

Equation 17 is obtained using the characteristics method in equation 7Ward and King (1997). Initial conditions are:

$$\hat{S}(0)=1,\qquad \hat{c}(\hat{r},0)=1,\qquad \hat{n}(\hat{r},0)=1 \tag{18}$$

As we can see, boundary conditions belong to the *moving boundary condition* Crank (1987) family of problems. In our case, the tumor radius acts as boundary and the growth of the tumor is driven by the velocity field following the equation 15.

3.2 Fixing the moving boundary

Before solving the system, the moving boundary is fixed by setting $\hat{r} = \hat{S}(t)r^*$. So let $r^* = \frac{\hat{r}}{\hat{S}(\hat{t})} \in [0,1]$. Then we must rewrite the differentials:

$$\frac{\partial \hat{n}(\hat{r},\hat{t})}{\partial \hat{t}} = \frac{\partial \hat{n}(r^*,\hat{t})}{\partial \hat{t}} + \left(\frac{\partial r^*}{\partial \hat{t}}\right)\frac{\partial \hat{n}(r^*,\hat{t})}{\partial r^*} = \frac{\partial \hat{n}(r^*,\hat{t})}{\partial \hat{t}} - \left(\hat{r}\frac{\partial \hat{S}}{\partial \hat{t}}\frac{1}{\hat{S}^2}\right)\frac{\partial \hat{n}(r^*,\hat{t})}{\partial r^*} =$$

$$= \frac{\partial \hat{n}(r^*,\hat{t})}{\partial \hat{t}} - \left(r^*\frac{\partial \hat{S}}{\partial \hat{t}}\frac{1}{\hat{S}}\right)\frac{\partial \hat{n}(r^*,\hat{t})}{\partial r^*}$$

$$\frac{\partial \hat{n}(\hat{r},\hat{t})}{\partial \hat{r}} = \underbrace{\frac{\partial \hat{t}}{\partial \hat{r}}}_{=0}\frac{\partial \hat{n}(r^*,\hat{t})}{\partial \hat{t}} + \frac{\partial r^*}{\partial \hat{r}}\frac{\partial \hat{n}(r^*,\hat{t})}{\partial r^*} = \frac{1}{\hat{S}}\frac{\partial \hat{n}(r^*,\hat{t})}{\partial r^*}$$

Applying the same transformations for $\hat{c}$ and $\hat{v}$ we obtain the system for $r^* \in [0,1]$:

$$\frac{\partial \hat{n}}{\partial \hat{t}} + \frac{\hat{v}(\hat{t},r^*) - r^*\hat{v}(\hat{t},1)}{\hat{S}}\frac{\partial \hat{n}}{\partial r^*} = [a(\hat{c}) - b(\hat{c})\hat{n}]\hat{n} \tag{19}$$

$$\frac{1}{r^{*2}}\frac{1}{\hat{S}}\frac{\partial (r^{*2}\hat{v})}{\partial r^*} = b(\hat{c})\hat{n} \tag{20}$$

$$\frac{1}{r^{*2}}\frac{1}{\hat{S}^2}\frac{\partial}{\partial r^*}\left(r^{*2}\frac{\partial \hat{c}}{\partial r^*}\right) = k(\hat{c})\hat{n} \tag{21}$$

3.3 Numerical Solution

The general scheme for the numerical solution is the one described in Ward and King (1997). Equations are sequentially solved by the finite-difference method Smith (1986) in a predictor-corrector scheme Gear (1971). The equation order is the following:

1. Tumour radius is updated by the outer velocity.
2. Nutrient concentration (eq. 21) is solved by a second-order accurate method.
3. The velocity equation (eq. 20) is approximated by the trapezium method Burden and Faires (1985).
4. Cell population (eq. 19) is calculated by the method described in Courant et al. (1952).

The system is initialized with the initial conditions mentioned before. The previous sequence is repeated at each time t, until convergence is achieved with a certain tolerance. We will use i for spatial-domain and j for time-domain iterations. We will set $F_i^j = F^j(x_i)$ as the function F evaluated in x_i at the time corresponding to iteration j. The mesh used to solve the system is a contracting mesh: $h_i = \lambda h_{i-1}$ for $i = 0, 1, ..., N$ with $0 < \lambda \leq 1$. k represents the time increment.

3.3.1 Tumour Radius

Tumor radius can be described by:

$$\int_{t_j}^{t_{j+1}} \frac{\partial S}{\partial t}\, dt = \int_{t_j}^{t_{j+1}} v(t,1)\, dt$$

As this is an ordinary differential equation the trapezium method can be used to obtain:

$$S^{j+1} = S^j + \frac{(v_N^{j+1} + v_N^j)\, k}{2} \tag{22}$$

3.3.2 Nutrient Concentration

The following equation belongs to the *two-point boundary equation* family:

$$\frac{\partial}{\partial r}\left(r^2 \frac{\partial c}{\partial r}\right) = r^2\, S^2\, k(c)\, n$$

We solve it by a second-order accurate finite-difference method:

$$\left(r_{i+\frac{1}{2}}^2 \frac{c_{i+1} - c_i}{h_i} - r_{i-\frac{1}{2}}^2 \frac{c_i - c_{i-1}}{h_{i-1}}\right) \frac{2}{h_i + h_{i-1}} = r_i^2\, S^2\, k(c_i)\, n_i$$

The boundary condition indicates that concentration at $r = 1$ is 1. Then we approximate the domain from $i = N$ to $i = 1$. At $r = 0$, the boundary condition determines that derivative is 0. So:

$$\begin{aligned}
&c_N = 1 \\
&c_i = \frac{\frac{1}{2}\, r_i^2\, s^2\, k(c_i)\, n_i\, (h_i + h_{i-1})\, h_i\, h_{i-1} - r_{i+\frac{1}{2}}^2\, h_{i-1}\, c_{i+1} - r_{i-\frac{1}{2}}^2\, h_i\, c_{i-1}}{-r_{i+\frac{1}{2}}^2\, h_{i-1} - r_{i-\frac{1}{2}}^2\, h_i} \quad \text{for } i = N-1, N-2, ..., 1 \\
&c_0 = \frac{(1+\lambda)^2 c_1 - c_2}{\lambda(\lambda+2)}
\end{aligned} \tag{23}$$

It is worth to notice that this is an implicit equation: c_i is involved in both sides of the equation. This is solved with the Newton's method Burden and Faires (1985).

3.3.3 Velocity

Velocity field can be described by:

$$\int_{r_i}^{r_{i+1}} \frac{\partial (r^2 v)}{\partial r}\, dr = \int_{r_i}^{r_{i+1}} r^2\, S\, b(c)\, n\, dr$$

Again, as this is an ordinary differential equation the trapezium method can be used. In this case, the boundary condition of cell velocity is at $r = 0$ so we can approximate the domain

from $i = 0$ to $i = N$ obtaining:

$$\begin{aligned} v_0 &= 0 \\ v_{i+1} &= \frac{1}{r_{i+1}^2}\left(r_i^2\, v_i + \left(\frac{(r_{i+1}^2\, S\, b(c_{i+1})\, n_{i+1} + r_i^2\, S\, b(c_i)\, n_i)\, h_i}{2}\right)\right) \quad \text{for } i = 0, 1, ..., N-1 \end{aligned} \tag{24}$$

3.3.4 Cell Population

Finally, we apply the method explained in Courant et al. (1952). The boundary condition sets the cell population at outer boundary so we approximate the domain from $i = N$ to $i = 0$.

$$\begin{aligned} \frac{n_i^{j+1} - n_i^j}{k} + \frac{v_i - r_i v_N}{S}\frac{n_{i+1} - n_i}{h_i} &= [a(c_i) - b(c_i)n_i]n_i \qquad \text{if } \frac{v_i - r_i v_N}{S} \leq 0 \\ \frac{n_i^{j+1} - n_i^j}{k} + \frac{v_i - r_i v_N}{S}\frac{n_i - n_{i-1}}{h_{i-1}} &= [a(c_i) - b(c_i)n_i]n_i \qquad \text{if } \frac{v_i - r_i v_N}{S} > 0 \end{aligned}$$

n_i^j are the values calculated in the previous time step while n_i, velocity and concentration values are the ones obtained in the previous iteration.

$$\begin{aligned} n_N &= \frac{a(1)e^{a(1)t}}{a(1) - b(1)(1 - e^{a(1)t})} \\ n_i^{j+1} &= \begin{cases} n_i^j + k\left((a(c_i) - b(c_i)n_i)n_i - \frac{v_i - r_i v_N}{S}\frac{n_{i+1} - n_i}{h_i}\right) & \text{if } \frac{v_i - r_i v_N}{S} \leq 0 \\ n_i^j + k\left((a(c_i) - b(c_i)n_i)n_i - \frac{v_i - r_i v_N}{S}\frac{n_i - n_{i-1}}{h_{i-1}}\right) & \text{if } \frac{v_i - r_i v_N}{S} > 0 \end{cases} \end{aligned} \tag{25}$$

4 LOCAL BEHAVIOR OF THE MODEL

If we insert Eq. 2 in the non-dimensionalizated dynamical Eqs. 1 and 3; we take off the divergence terms; and we fix $m_1 = m_2 = 1$, $A = 1$ and $c_d = c_e$; we arrive to the following system:

$$\frac{\partial n}{\partial t} = -n^2\left(\frac{c}{c+d} - (1-\delta)(1 - \sigma\frac{c}{c+d})\right) + n\left((1+\sigma)\frac{c}{c+d} - 1\right) \tag{26}$$

$$\frac{\partial c}{\partial t} = -c\, n\left(\frac{c}{c+d} - (1-\delta)(1 - \sigma\frac{c}{c+d}) - c\beta\frac{c}{c+d} - c\gamma\right) \tag{27}$$

If we search fixed points in the phase space (n, c), we find a trivial solution at $(n, c = 0)$. As $c = 0$, there are no cells in the system so we obtain a constant behavior. On the other hand, we find two more solutions: $(n+, c+)$ and $(n-, c-)$, corresponding to two non-trivial fixed points:

$$n_\pm = \frac{\sigma c_\pm - d}{c_\pm - (1-\delta)(d + c_\pm(1-\sigma))} \tag{28}$$

$$c_\pm = \frac{(\beta + \gamma - d(1-\delta)) \pm \sqrt{(\beta + \gamma - d(1-\delta))^2 - 4d\gamma(\delta + (1-\delta)\sigma)}}{-2(\delta + (1-\delta)\sigma)} \tag{29}$$

Seting $\sigma = 0.9$, $\delta = 0.5$ and $d = 0.1$, we move the parameters β and γ to make the analysis of local dynamics.

Fixing $\beta = 0.05$, but in general for any value of this parameter, we find variating γ that the two fixed points define two branches: one stable and one unstable (figure 2).

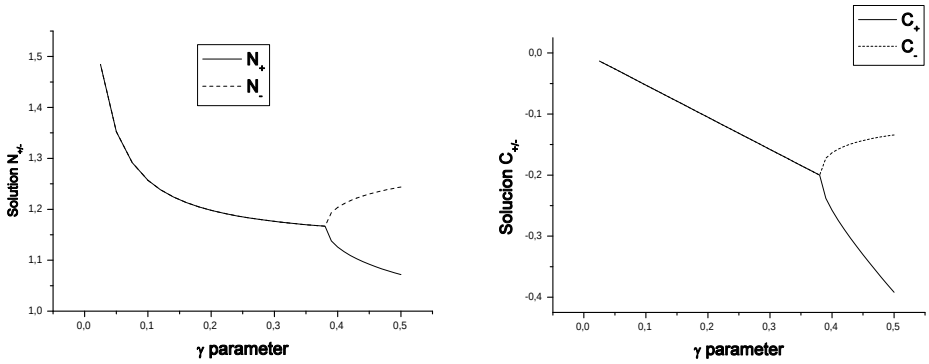

Figure 2: Local behavior for n and c, $\beta = 0.05$, $\sigma = 0.9$, $\delta = 0.5$ and $d = 0.1$. $\gamma = 0.38$ defined where the real eigenvalues join into conjugated values. For greater values we observe two branches: solid and dotted lines show stable and unstable branches, respectively. For smaller values, the real part coincides while imaginary part differs, defining a Hopf bifurcation.

If we set γ greater than 0.38, both fixed points are real and the evolution of the system into the phase space shows that it falls into a stable solution (figure 3).

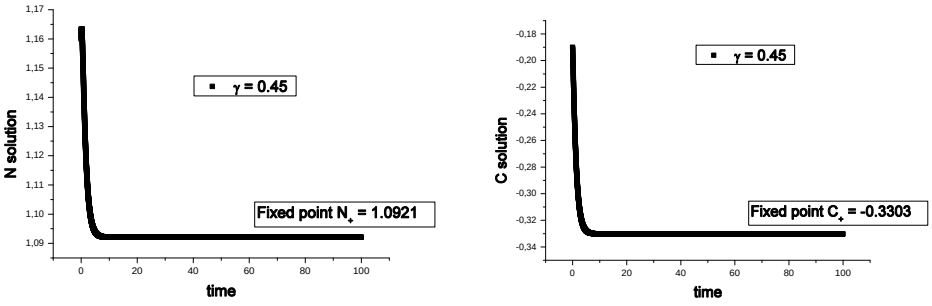

Figure 3: Local behavior for n and c, $\beta = 0.05$, $\sigma = 0.9$, $\delta = 0.5$, $d = 0.1$ and $\gamma = 0.45$. With $\gamma > 0.38$, the system falls to stable solution.

On the contrary, if we set γ smaller than 0.38, both fixed points become complex conjugates and the evolution of the system presents an oscillatory behavior typical of a Hofp bifurcation (figure 4).

Figure 5 presents a successive zooming of the solution trajectory around the fixed points and it reveals a chaotic behavior.

5 NUMERICAL RESULTS

The mesh used for solving the system was a 100-step contracting mesh, with $\lambda = 0.95$. Normal and border values for the physically motivated parameters Ward and King (1997) are shown in table 1.

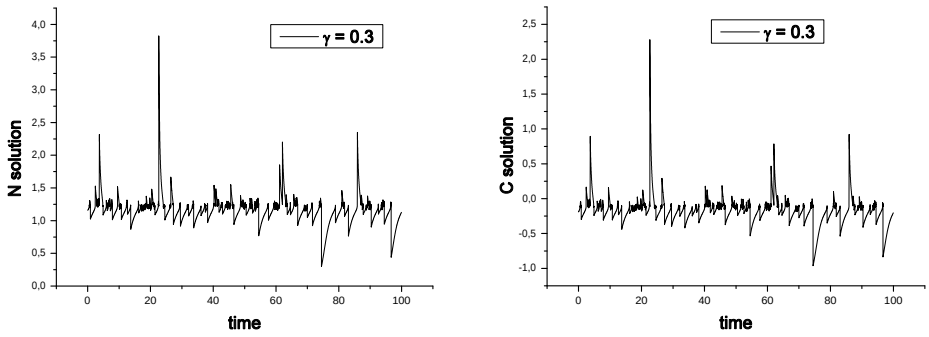

Figure 4: Local behavior for n and c, $\beta = 0.05$, $\sigma = 0.9$, $\delta = 0.5$, $d = 0.1$ and $\gamma = 0.3$. With $\gamma < 0.3$, the solution oscillates around fixed points.

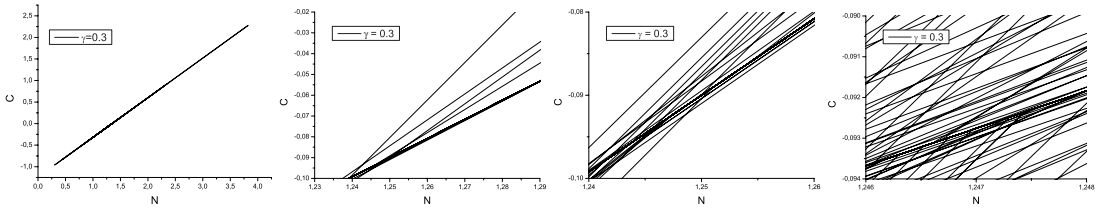

Figure 5: Local behavior for n and c, $\beta = 0.05$, $\sigma = 0.9$, $\delta = 0.5$, $d = 0.1$ and $\gamma = 0.3$. Zoom into the phase space of the solution show chaotic behaviour.

Note: Extreme values of β, c_c and c_d presented in this table correspond to the upper and lower limiting curves exposed in Figure 6 and are in good agreement with the experimental results obtained in Conger and Ziskin (1983); Li (1982).

Figure 6 shows the dimensionless tumor radius for three different parameter values. As appointed in bibliography, we observe an initial period in which the rate of growth increases, then it slows down (although barely noticeably in the graph) and finally becomes constant Conger and Ziskin (1983); Freyer and Sutherland (1986); Koch et al. (1973).

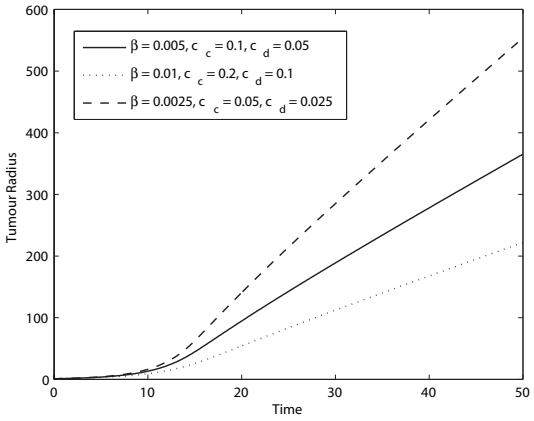

Figure 6: The dimensionless tumor radius, S(t), plotted against time for different parameter values

For averaged parameter values the velocity of tumor growth obtained is $2\mu m/h$. For other possible values, we arrive to faster ($3\mu m/h$) or slower ($1\mu m/h$) tumor growth velocities.

Table 1: Parameter values for different tumour growth velocities.

Parameter	Normal Growth	Slow Growth	Fast Growth
σ	0.9		
δ	0.5		
β	0.005	0.01	0.0025
c_c	0.1	0.2	0.05
c_d	0.05	0.1	0.025
$m_1 = m_2$	1		
B/A	1		
γ	0		

5.1 Shrinking to a necrotic core

It is stated that if the natural death rate of living cells is larger than their proliferation rate then the tumor shrinks to a necrotic core Tao and Miaojun (2006). Clearly, if σ and δ are small enough then this condition holds and we may expect that the living cells will eventually die. Under this assumptions, the numerical solution showed a decreasing tumor radius toward a necrotic core. In figure 7 we can observe how the tumor shrinks to a necrotic core due to living cell depletion.

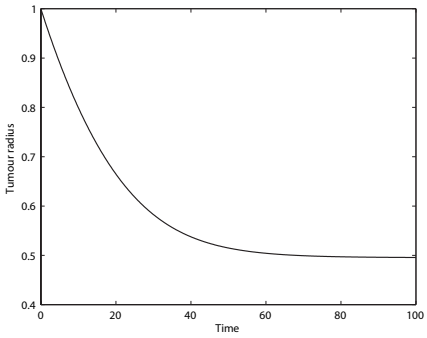

Figure 7: Tumor shrinking to a necrotic core.

6 DISCUSSION

Cancer development modeling is a complex issue that has been widely explored in recent years resulting in the production of numerous mathematical models with different approaches. Many previous models of tumor growth represent the tumor as a mass with discrete inner layers separated by moving boundaries. Recently, nevertheless, there have appeared new models formulated in terms of continuum densities of proliferating, quiescent and necrotic cells. These models seem to be in many cases numerically more efficient, which result in more accurate simulations of reality Schaller and Meyer-Hermann (2006); Sherratt and Chaplain (2001). Ward's models are continuum models based in partial differential equations that describe the growth or regression of avascular microtumors in response to the nutrient and/or drug concentration present in the medium. Proliferation or death of tumor cells implies the expansion or contraction of the tumor volume, respectively, with the consequent generation of an associated velocity field.

Resolution of the mathematical model results in one of three long-term stable possible solutions: the trivial solution (tumor death), the traveling wave solution (continuous tumor growth) and a sub linear growth case in which cells reach a pseudo-steady-state in the core. It has been recently theoretically proved that this model (that implies a free boundary problem Crank (1987)) has a unique global solution Tao and Miaojun (2006). Under specific initial conditions and natural assumptions on model parameters, this global solution converges to a trivial steady-state of tumor death. This kind of model can be experimentally applied to and validated by the biological model of multicellular spheroids, which is at present considered the optimum in vitro model to study complex aspects of avascular tumor development Kunz-Schughart et al. (2004).

In this paper we explicitly detailed a numerical method to extent the mathematical model previously proposed by Ward. His work applied a single set of parameter values, therefore a single curve was calculated. In contrast, we present a range of feasible solutions for tumor growth, depending on different possible biological responses corresponding to different tumor cell lines. This covers a more realistic scenario. We also analyzed the local dynamics of the model, and found a chaotic behavior for a specific set of parameter values. This may represent an interesting issue to be studied more deeply, both mathematically and experimentally. Finally, our work validated numerically analytical works previously presented by others Tao and Miaojun (2006).

Characterization of tumor growth kinetics in terms of clinically relevant parameters is increasingly required in the optimization and personalization of treatments. The design of mathematical and computational models employing parameter values in the physiological range of operation, together with its experimental validation, has the future perspective of its upgrade and utilization in the modeling of different therapeutic strategies against the development of avascular microtumors and micrometastasis.

ACKNOWLEDGEMENTS

GM, MR and CS are investigators at the National Research Council of Argentina (CONICET). AS is supported by CNEA and University of Buenos Aires (UBA). DFS is supported by YPF Foundation and UBA.

REFERENCES

Burden R. and Faires J. *Numerical analysis*. Prindle, Weber & Schmidt Boston, Mass, 1985.

Byrne H., Alarcon T., Owen M., Webb S., and Maini P. Modelling aspects of cancer dynamics: a review. *Philos Transact A Math Phys Eng Sci*, 364(1843):1563–1578, 2006.

Casciari J., Sotirchos S., and Sutherland R. Variation in tumour cell growth rates and metabolism with oxygen-concentration, glucose-concentration and extracellular ph. *J Cell Physiol*, 151:386–394, 1992.

Conger A. and Ziskin M. Growth of mammalian multicellular tumour spheroids. *Cancer Research*, 43:558–560, 1983.

Courant R., Isaacson E., and Rees M. On the solution of nonlinear hyperbolic differential equations by finite difference. *Communications on Pure and Applied Mathematics*, 5:243–255, 1952.

Crank J. *Free and Moving Boundary Problems*. Oxford University Press, USA, 1987.

Freyer J. and Sutherland R. Regulation of growth saturation and development of necrosis in emt6/ro multicellular spheroids by the glucose and oxygen supply. *Cancer Research*, 46(7):3504–3512, 1986.

Gear C. *Numerical Initial Value Problems in Ordinary Differential Equations*. Prentice Hall PTR Upper Saddle River, NJ, USA, 1971.

Hlatky L., Suchs R., and Alpen E. Joint oxygen-glucose deprivation as the cause of necrosis in a tumour analogue. *J Cell Phys*, 134:167–178, 1988.

Koch C., Kruuv J., and Frey H. The effect of hypoxia on the generation time of mammalian cells. *Radiat Res*, 53(1):43–8, 1973.

Kunz-Schughart L., Freyer J., Hofstaedter F., and Ebner R. The use of 3-d cultures for high-throughput screening: the multicellular spheroid model. *J Biomol Screen*, 9 (4):273–285, 2004.

Li C. The glucose distribution in 9l rat brain multicell tumour spheroids and its effect on cell necrosis. *Cancer*, 50:2066–2073, 1982.

Preziosi L., editor. *Cancer Modelling and Simulation*. CHAPMAN & HALL/CRC, London, UK, 2003.

Schaller G. and Meyer-Hermann M. Continuum versus discrete model: a comparison for multicellular tumour spheroids. *Philos Transact A Math Phys Eng Sci*, 364(1843):1443–1464, 2006.

Sherratt J. and Chaplain M. A new mathematical model for avascular tumour growth. *J Math Biol*, 43 (4):291–312, 2001.

Smith G. *Numerical Solution of Partial Differential Equations: Finite Difference Methods*. Oxford University Press, 1986.

Tao Y. and Miaojun C. An elliptic-hyperbolic free boundary problem modelling cancer therapy. *Nonlinearity*, 19:419–440, 2006.

Ward J. and King J. Mathematical modelling of avascular-tumour growth. *IMA J Math Appl Med Biol*, 14 (1):39–69, 1997.

Ward J. and King J. Mathematical modelling of avascular-tumour growth ii: Modelling growth saturation. *IMA J Math Appl Med Biol*, 16 (2):171–211, 1999.

Ward J. and King J. Mathematical modelling of drug transport in tumour multicell spheroids and monolayer cultures. *Math Biosci*, 181 (2):177–207, 2003.